

Elongated Dihydrogen Complexes: A Combined Electronic DFT + Nuclear Dynamics Study of the $[\text{Ru}(\text{H}\cdots\text{H})(\text{C}_5\text{H}_5)(\text{H}_2\text{PCH}_2\text{PH}_2)]^+$ Complex

Ricard Gelabert, Miquel Moreno, José M. Lluch,* and Agustí Lledós*

Contribution from the Departament de Química, Universitat Autònoma de Barcelona, 08193 Bellaterra, Barcelona, Spain

Received March 14, 1997. Revised Manuscript Received July 25, 1997[⊗]

Abstract: A study on a modeled version of the complex $[\text{Ru}(\text{H}\cdots\text{H})(\text{C}_5\text{Me}_5)(\text{dppm})]^+$ has been performed both at electronic structure level and including quantum treatment of nuclei. Density functional theory (DFT) electronic structure calculations alone fail to reproduce the experimentally reported geometry of the elongated dihydrogen ligand of the complex, even though the rest of the complex is satisfactorily described. Quantum nuclear motion calculations manage to correctly explain the geometries found experimentally by means of neutron diffraction measurements. Isotopic effects are predicted for the hydrogen–hydrogen distance of the elongated dihydrogen ligand depending on its isotopic composition. Moreover, the temperature dependence of the $J(\text{H},\text{D})$ coupling constant is also interpreted successfully on the grounds of varying population of the vibrational excited states of the $\text{Ru}-\text{H}_2$ unit.

I. Introduction

The complexes which present hydrogen atoms in the coordination sphere of the metal are currently being classified into two large groups: those in which the distance between hydrogen atoms exceeds 1.6 Å, which have been known for a long time and are referred as classical polyhydrides in the literature, and those in which this same distance has a value between 0.8 and 1.0 Å, first discovered by Kubas and which have been known as “non-classical dihydrogen complexes”.¹ The difference between both types of complexes has faded with time due to the discovery of a series of complexes whose H–H distances fall between the two above mentioned limits.^{1c} These complexes, known as elongated dihydrogen complexes, have been found both in solution and in solid-state structures. They have been characterized in solution by means of $T_1(\text{min})$ and $J(\text{H},\text{D})$ coupling ¹H NMR measurements while in the solid-state they have been characterized by means of ¹H NMR, X-ray diffraction, and neutron diffraction studies.^{2–5}

In solution, values of $T_1(\text{min})$ between 6 and 90 ms at 200 MHz have been indicative of these elongated dihydrogen structures.^{1c} $T_1(\text{min})$ values are, however, directly proportional to the observation frequencies, and hence this range should be scaled accordingly when comparing data coming from different experiments. Be it as it may, $T_1(\text{min})$ values lead to ambiguous

values for the H–H distance depending on the interpretation of the motion of the H_2 unit in the complex.^{5b,6} A better estimate of the H–H distance in solution can be obtained through the study of $J(\text{H},\text{D})$ coupling constants.^{1d,5–7} It is known that for free HD the $J(\text{H},\text{D})$ coupling constant has a value of 43 Hz. Careful quantum chemical studies have shown that the coupling constant in free H_2 increases with H–H distance, although it decays to zero in the limit of complete dissociation.⁸ This seems to indicate that $J(\text{H},\text{D})$ for elongated dihydrogen complexes should be greater than 43 Hz. However, it has been proposed that values of $J(\text{H},\text{D})$ coupling between 5 and 25 Hz denote a stretched dihydrogen complex.^{1c} It seems surprising that values such as these could correspond to any form of bound dihydrogen. Anyway, a very recent quantum chemical calculation of $J(\text{H},\text{D})$ coupling constant using density functional theory (DFT) has shown that the diminished value of $J(\text{H},\text{D})$ in elongated dihydrogen complexes is a consequence of the increasing metal–hydrogen bond strength.^{7b} Further, a good linear correlation between $J(\text{H},\text{D})$ coupling constants and H–H distances was found by Maltby *et al.* for a series of dihydrogen complexes whose structures have been determined by means of neutron diffraction, X-ray diffraction or solid-state NMR techniques:^{5b}

$$d_{\text{H-H}} = 1.42 - 0.0167J(\text{H},\text{D}) \quad (1)$$

where it has been implicitly assumed that the distance between hydrogen isotopes is not affected by the nature of the isotopic substitution. In this equation $J(\text{H},\text{D})$ comes in hertz, and $d_{\text{H-H}}$ in ångströms. A similar connection between $J(\text{H},\text{D})$ and $d_{\text{H-H}}$ has been pointed out by Heinekey and Luther.^{5c}

In solid-state, direct measurements of H–H distances can be carried out by neutron diffraction, which can be considered the most precise technique for the resolution of crystallographic data

[⊗] Abstract published in *Advance ACS Abstracts*, September 15, 1997.

(1) (a) Kubas, G. J. *Acc. Chem. Res.* **1988**, *21*, 120. (b) Crabtree, R. H. *Acc. Chem. Res.* **1990**, *23*, 95. (c) Jessop, P. J.; Morris, R. H. *Coord. Chem. Rev.* **1992**, *121*, 155. (d) Heinekey, D. M.; Oldham, W. J., Jr. *Chem. Rev.* **1993**, *93*, 913. (e) Crabtree, R. H. *Angew. Chem., Int. Ed. Engl.* **1993**, *32*, 789.

(2) Brammer, L.; Howard, J. A. K.; Johnson, O.; Koetzle, T. F.; Spencer, J. L.; Stringer, A. M. *J. Chem. Soc., Chem. Commun.* **1991**, 241.

(3) Albinati, A.; Bakhmutov, V. I.; Caulton, K. G.; Clot, E.; Eckert, J.; Eisenstein, O.; Gusev, D. G.; Grushin, V. V.; Hauger, B. E.; Klooster, W. T.; Koetzle, T. F.; McMullan, R. K.; O’Loughlin, T. J.; Pélissier, M.; Ricci, J. S.; Sigalas, M. P.; Vymenits, A. B. *J. Am. Chem. Soc.* **1993**, *115*, 7300.

(4) Hasegawa, T.; Li, Z.; Parkin, S.; Hope, H.; McMullan, R. K.; Koetzle, T. F.; Taube, H. *J. Am. Chem. Soc.* **1994**, *116*, 4352.

(5) (a) Klooster, W. T.; Koetzle, T. F.; Jia, G.; Fong, T. P.; Morris, R. H.; Albinati, A. *J. Am. Chem. Soc.* **1994**, *116*, 7677. (b) Maltby, P. A.; Schlaf, M.; Steinbeck, M.; Lough, A. J.; Morris, R. H.; Klooster, W. T.; Koetzle, T. F.; Srivastava, R. C. *J. Am. Chem. Soc.* **1996**, *118*, 5396. (c) Heinekey, D. M.; Luther, T. A. *Inorg. Chem.* **1996**, *35*, 4396.

(6) (a) Schlaf, M.; Lough, A. J.; Maltby, P. A.; Morris, R. H. *Organometallics* **1996**, *15*, 2270. (b) Gusev, D. G.; Kuhlman, R. L.; Renkema, K. B.; Eisenstein, O.; Caulton, K. G. *Inorg. Chem.* **1996**, *35*, 6775.

(7) (a) Craw, J. S.; Bacskey, G. B.; Hush, N. S. *J. Am. Chem. Soc.* **1994**, *116*, 5937. (b) Bacskey, G. B.; Bytheway, I.; Hush, N. S. *J. Am. Chem. Soc.* **1996**, *118*, 3753.

(8) Bacskey, G. B. *Chem. Phys. Lett.* **1995**, *242*, 507.

that presently exists. However, due to the rapid librational motion of the H₂ unit in the dihydrogen complexes (elongated or otherwise), H–H dihydrogen distances coming directly from neutron diffraction experiments are artificially short and need to be corrected to account for this librational motion. Once this correction has been taken into account, it can be seen that these elongated dihydrogen complexes cover a wide range of H–H distances: [Ru(H···H)(C₅Me₅)(dppm)]BF₄ (1.10 Å),^{5a} *cis*-[Ir(H···H)HCl₂(PⁱPr₃)₂] (1.11 Å),³ [Os(H···H)Cl(dppe)₂]PF₆ (1.22 Å),^{5b} [Os(H···H)(en)₂(OAc)]PF₆ (1.34 Å),⁴ and [Re(H···H)(H)₅(Ptol₃)₂] (1.357 Å).²

Some unusual behavior with respect to the temperature dependence of *J*(H,D) coupling has been discovered for the few cases of elongated dihydrogen complexes in which detailed NMR studies have been carried out. To our knowledge, only three complexes have been studied in this way: [Ru(H···D)(C₅Me₅)(dppm)]⁺,^{5a} *trans*-[Os(H···D)H(dppe)₂]⁺,⁹ and *trans*-[Os(H···D)Cl(dppe)₂]⁺.^{5b} Several different explanations for this temperature dependence of the *J*(H,D) coupling constant have been proposed. The first attempt to explain this unusual temperature dependence was founded on the grounds that there was no such thing as an elongated dihydrogen complex but, instead, a rapid interconversion of spinning dihydrogen and dihydride tautomers whose equilibrium constant was temperature dependent.⁹ The different *J*(H,D) coupling values obtained at different temperatures would come from different compositions of the equilibrium mixtures between both tautomers. Elegant as it may seem, this hypothesis had to be ruled out because in the solid-state, at very low temperatures, neutron diffraction studies still detected only an elongated dihydrogen structure. At those temperatures the equilibrium would be completely displaced toward the most stable of both tautomers. A different explanation, proposed by Klooster *et al.* ascribed the temperature dependence of the *J*(H,D) coupling constant to differences in the population of the vibrational excited states of the H₂ unit.^{5a} The assumption is that the higher in energy a state is, the longer the H–D (H–H) distance becomes. At higher temperatures the population of the excited states would increase, which would produce a longer mean H–D distance, and consequently, the *J*(H,D) coupling values would become lower. Within this hypothesis, the elongated dihydrogen structure would have real existence as a more or less shallow minimum in the global potential energy surface. While this would qualitatively explain the behavior of the complex [Ru(H···H)(C₅Me₅)(dppm)]⁺, it fails to explain that of the osmium complexes. In these, *J*(H,D) coupling constants increase with increasing temperature, a fact that within this hypothesis would indicate that the vibrational excited states for these two complexes have *shorter* H–H (H–D) distances. Finally, in a more recent work Maltby *et al.*, while studying the complex *trans*-[Os(H···H)Cl(dppe)₂]⁺, again discard the equilibrium hypothesis and suggest an explanation based on the rapid motion of two hydrogen atoms in a flat potential energy surface with a shallow minimum at the crystallographically determined position where the H–H distance is about 1.2 Å.^{5b} To summarize, it seems that, up to now, there is no overall explanation able to justify the different temperature behavior of *J*(H,D) coupling in this particular kind of dihydrogen complexes.

Despite the great quantity of theoretical studies on molecular hydrogen complexes,^{7,10} there are very few dealing with

elongated dihydrogen complexes.^{11–13} However, no satisfactory theoretical explanation of the existence of these elongated dihydrogen complexes has been found yet. In this paper we have set our objectives in the study of one of the three elongated dihydrogen complexes for which there is information of the temperature dependence of *J*(H,D) coupling constant: the complex [Ru(H···H)(C₅Me₅)(dppm)]BF₄.^{5a} To achieve this, a DFT study of the potential energy surface of this complex will be carried out to check the existence of this hypothetical shallow minimum. Moreover, we will try to explain the temperature dependence of the *J*(H,D) coupling constant for this particular complex. To this end, nuclear wave function calculations will be carried out to find the vibrational levels and their corresponding wave functions.

II. Computational Details

As stated in the Introduction, a part of this work is concerned with obtaining the temperature dependence of the coupling constant *J*(H,D). To achieve this, calculations have been carried out to obtain vibrational energy levels. Two different kinds of calculations have been carried out: electronic structure calculations, meant to locate the hypothetical shallow minimum on the entire potential energy surface (PES) corresponding to the complex under study, and characterization of other relevant stationary points, and nuclear motion calculations, aimed at obtaining the corresponding energy levels and wave functions. Both sets of calculations are explained below.

A. Electronic Structure Calculations. The complex under study was modeled somewhat by turning the C₅Me₅ unit into a cyclopentadienyl (C₅H₅) ligand and by substituting the four phenyl groups in the dppm (dppm = bis(diphenylphosphino)methane) ligand by four hydrogen atoms. Hence, the system finally studied was the cationic complex [Ru(H₂)(C₅H₅)(H₂-PCH₂PH₂)]⁺. Even though the size of the modeled system is not too large, great care has to be taken to choose the right methodology and underlying basis set to solve the electronic Schrödinger equation. Apart from the localization of stationary points, a reduced potential energy surface had to be evaluated with the same methodology. This means that apart from choosing the methodology based on accuracy considerations, the methodology used should allow the calculation of this reduced PES in a reasonable amount of time. Fortunately, theoretical organometallic chemistry has at its disposal a relatively new formalism that, apart from having been tested on a plethora of interesting problems with amazing success, fulfills the requirements of speed and accuracy needed for the construction of a sizeable portion of the PES of the system. This formalism is the density functional theory (DFT).¹⁴

In all calculations performed, full geometry optimizations have been carried out by imposing global symmetry C₅. All electronic structure calculations were carried out with the

(10) Some theoretical studies on dihydrogen complexes: (a) Jean, Y.; Eisenstein, O.; Volatron, F.; Maoche, B.; Sefta, F. *J. Am. Chem. Soc.* **1986**, *108*, 6587. (b) Hay, P. J. *J. Am. Chem. Soc.* **1987**, *109*, 705. (c) Maseras, F.; Duran, M.; Lledós, A.; Bertrán, J. *J. Am. Chem. Soc.* **1991**, *113*, 2879. (d) Dapprich, S.; Frenking, G. *Angew. Chem., Int. Ed. Engl.* **1995**, *34*, 354. (e) Li, J.; Ziegler, T. *Organometallics* **1996**, *15*, 3844.

(11) Maseras, F.; Lledós, A.; Costas, M.; Poblet, J. M. *Organometallics* **1996**, *15*, 2947.

(12) Lin, Z.; Hall, M. B. *Coord. Chem. Rev.* **1994**, *135–136*, 845.

(13) Craw, J. S.; Bacskay, G. B.; Hush, N. S. *Inorg. Chem.* **1993**, *32*, 2230.

(14) Parr, R. G.; Yang, W. *Density-Functional Theory of Atoms and Molecules*; Oxford University Press: Oxford, U.K., 1989.

(9) Earl, K. A.; Jia, G.; Maltby, P. A.; Morris, R. H. *J. Am. Chem. Soc.* **1991**, *113*, 3027.

GAUSSIAN 94 series of programs,¹⁵ and the DFT formalism was used throughout the entire process with the three-parameter hybrid functional of Becke and the Lee, Yang, and Parr's correlation functional, widely known as Becke3LYP.¹⁶

An effective core operator was used to replace the inner electrons of the ruthenium atom, in this way eliminating 28 electrons from the system.¹⁷ For the remaining electrons of this atom, the basis set associated with the pseudopotential of Hay and Wadt¹⁷ with a standard valence double- ζ LANL2DZ contraction was used.¹⁵ As for the rest of atoms, the standard split-valence 6-31G basis set was chosen,^{18a} except for the phosphorous atoms, for which the basis set 6-31G(d) was used,^{18b} and the hydrogen atoms directly bound to the metal, for which the basis set used was 6-31G(p).^{18a,c}

In some cases, Becke3LYP calculations were carried out again with an enhanced basis set which added an f shell on the ruthenium atom^{18d} and d basis functions on all carbon atoms of the system.^{18a-c} Finally, higher level calculations were carried out in a few cases to account for additional electronic correlation. This was done by means of coupled cluster calculations involving single, double, and perturbatively triple excitations (CCSD(T)).¹⁹

B. Nuclear Motion Calculations. In order to determine both the energy levels and wave functions corresponding to the nuclear movement, the nuclear Schrödinger equation has to be solved:

$$[\hat{T}_{\text{nuc}} + U(\mathbf{R})]\Psi_{\text{nuc}} = E\Psi_{\text{nuc}} \quad (2)$$

where \mathbf{R} is a $3N - 6$ component vector whose elements describe a given nuclear geometry, and U is the electronic potential energy surface including the internuclear repulsion obtained within the Born–Oppenheimer approximation from the electronic structure calculations. Of course, evaluation of the whole $U(\mathbf{R})$ is a completely unattainable task except for the simplest of molecules. As has been already stated, the main concern of this work lies on the dynamics of the H_2 unit of the complex under study. With this in mind, the complexity of the problem has been simplified by reducing the dimensionality of the whole hypersurface to just two dimensions. These dimensions, or variables for U , had to be chosen with care if the expression of the kinetic energy operator in (2) was to be simple. Concretely, the two coordinates chosen to carry out the PES scan were the distance between both hydrogens and the distance between the metal center and the point halfway between the two hydrogen atoms in the dihydrogen ligand. These two parameters behave as orthogonal coordinates, in such a way that no coupled terms between them appear in the nuclear kinetic operator in (2). When calculating the PES, global relaxation of the rest of geometrical

parameters was allowed. Some additional details concerning the evaluation of the PES are given in the next section.

To solve (2) a discrete variable representation (DVR) has been used.²⁰ This method has already been used with success in problems of quantum mechanical reactive scattering²¹ and to determine vibrational states for small systems.²² Computationally, the DVR has great advantages over the more traditional variational basis representation (VBR), in which the energy levels are obtained by diagonalization of the matrix representation of the projection of the Hamiltonian operator on a given basis set, usually made up of Gaussian functions. In a few words, the primary difference between the finite basis representation lies in the fact that the DVR is a grid-point representation instead of a basis set representation, and thus it eliminates the need to evaluate the potential energy integrals V_{ij} , basically because there are no integrals to evaluate. In this representation, the potential energy matrix representation is diagonal and the kinetic energy matrix representation is very simple, yielding very sparse Hamiltonian matrices easier to diagonalize than those coming from a finite basis representation. This becomes very important when dealing with multidimensional problems in which the Hamiltonian matrices easily become huge. In this paper, the generic DVR proposed by Colbert and Miller has been used.^{20b} We present in this paper a DVR application to a real problem in the field of organometallic chemistry.

As a result of diagonalizing the grid-point representation of the Hamiltonian in (2), the eigenvalues (nuclear energy levels) and eigenvectors (nuclear wave function expanded as a linear combination of basis functions) are obtained. Within this particular DVR, the wave function associated to a given eigenvalue can be obtained as

$$\Psi_i = \sum_{j=1}^{N_p} c_{ij} \phi_j \quad (3)$$

where N_p is the total number of points in the grid. In a general two-dimensional case whose two dimensions are labeled x and y , ϕ_j are functions of the form

$$\phi_j(x,y) = \frac{\sin\left(\frac{\pi(x-x_m)}{\Delta x}\right)}{\pi(x-x_m)} \frac{\sin\left(\frac{\pi(y-y_n)}{\Delta y}\right)}{\pi(y-y_n)} \quad (4)$$

being x_m and y_n the (x,y) coordinates of the grid point associated with the coefficient j , and Δx and Δy the spacings in the x and y directions of the grid. The wave function has to be normalized prior to any calculation involving it. A more thorough methodological discussion concerning the PES construction and the DVR performance (especially in comparison with the traditional VBR representation) will be given elsewhere in a more technical report.

III. Results and Discussion

The first part of this section is concerned with the results coming from pure electronic structure analysis. The main goal of this study has been to carry out a thorough study of the PES of the complex trying to check the existence of the hypothetical shallow minimum proposed in the literature. In the second part,

(20) (a) Light, J. C.; Hamilton, I. P.; Lill, J. V. *J. Chem. Phys.* **1985**, *82*, 1400. (b) Colbert, D. T.; Miller, W. H. *J. Chem. Phys.* **1992**, *96*, 1982.

(21) See, among others: (a) Heather, R. W.; Light, J. C. *J. Chem. Phys.* **1983**, *79*, 147. (b) Lill, J. V.; Parker, G. A.; Light, J. C. *J. Chem. Phys.* **1986**, *85*, 900.

(22) See for instance: (a) Bačić, Z.; Light, J. C. *J. Chem. Phys.* **1986**, *85*, 4594. (b) Whitnell, R. M.; Light, J. C. *J. Chem. Phys.* **1989**, *90*, 1774.

(15) Frisch, M. J.; Trucks, G. W.; Schlegel, H. B.; Gill, P. M. W.; Johnson, B. G.; Robb, M. A.; Cheeseman, J. R.; Keith, T. A.; Petersson, G. A.; Montgomery, J. A.; Raghavachari, K.; Al-Laham, M. A.; Zakrzewski, V. G.; Ortiz, J. V.; Foresman, J. B.; Cioslowski, J.; Stefanov, B. B.; Nanayakkara, A.; Challacombe, M.; Peng, C. Y.; Ayala, P. Y.; Chen, W.; Wong, M. W.; Andres, J. L.; Replogle, E. S.; Gomperts, R.; Martin, R. L.; Fox, D. J.; Binkley, J. S.; Defrees, D. J.; Baker, J.; Stewart, J. P.; Head-Gordon, M.; Gonzalez, C.; Pople, J. A. *Gaussian 94*; Gaussian Inc.: Pittsburgh, PA, 1995.

(16) (a) Lee, C.; Yang, W.; Parr, R. G. *Phys. Rev. B* **1988**, *37*, 785. (b) Becke, A. D. *J. Chem. Phys.* **1993**, *98*, 5648.

(17) Hay, P. J.; Wadt, W. R. *J. Chem. Phys.* **1985**, *82*, 299.

(18) (a) Hehre, W. J.; Ditchfield, R.; Pople, J. A. *J. Chem. Phys.* **1972**, *56*, 2257. (b) Francl, M. M.; Pietro, W. J.; Hehre, W. J.; Binkley, J. S.; Gordon, M. S.; Defrees, D. J.; Pople, J. A. *J. Chem. Phys.* **1982**, *77*, 3654. (c) Hariharan, P. C.; Pople, J. A. *Theoret. Chim. Acta* **1973**, *28*, 213. (d) Ehlers, A. W.; Böhme, M.; Dapprich, S.; Gobbi, A.; Höllwarth, A.; Jonas, V.; Köhler, K. F.; Stegmann, R.; Veldkamp, A.; Frenking, G. *Chem. Phys. Lett.* **1993**, *208*, 111.

(19) (a) Bartlett, R. J. *J. Phys. Chem.* **1989**, *93*, 1697. (b) Bartlett, R. J.; Watts, J. D.; Kucharski, S. A.; Noga, J. *Chem. Phys. Lett.* **1990**, *165*, 513.

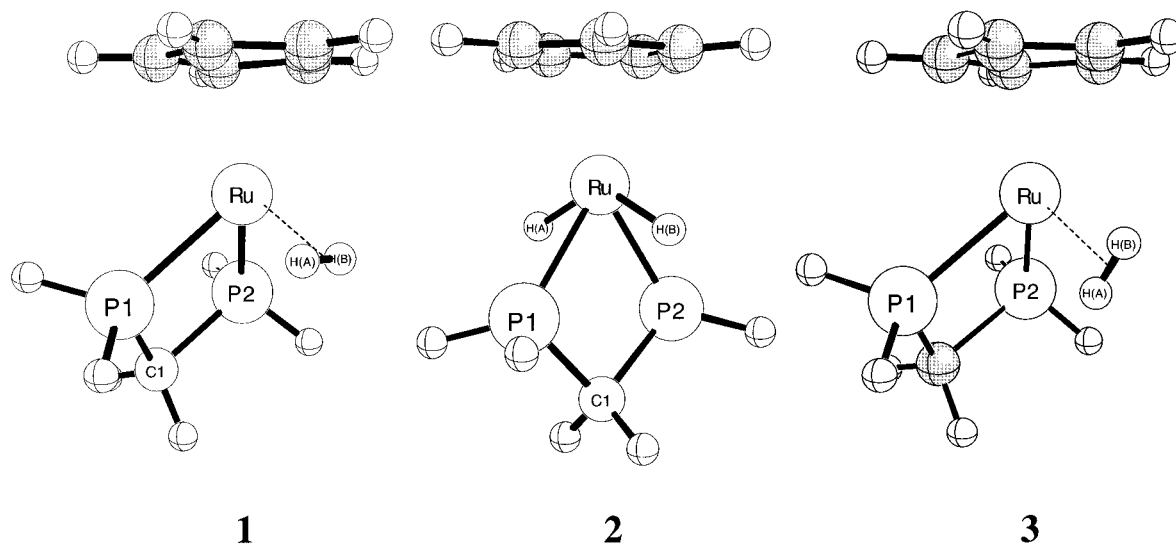


Figure 1. Optimized structures for the dihydrogen (1) and *trans*-dihydride (2) and the transition-state structure for the rotation of the dihydrogen unit of the dihydrogen complex (3).

nuclear motion studies devoted to determining the vibrational energy levels and wave functions are presented.

A. Electronic Structure Results. There have been experimental reports that state that for complexes of the form $[\text{RuH}_2(\text{C}_5\text{H}_5)(\text{diphosphine})]^+$ different isomers are obtained depending on the length of the hydrocarbon chain of the diphosphine chelating ligand n .^{23–25} In this way it has been seen that when $n = 3$ only a *trans*-dihydride is formed, whereas when $n = 1$ (the ligand is, then, dpmm) only the $\eta^2\text{-H}_2$ isomer is detected. In the case $n = 2$ a mixture of both isomers is formed in proportion 2:1, with the *trans*-dihydride structure being the most abundant.^{23–25} Chinn and Heinekey determined that for complexes of the type $[\text{Ru}(\text{C}_5\text{H}_5)\text{H}(\text{R}_2\text{P}(\text{CH}_2)_2\text{PR}'_2)]$ the sole product of the protonation at 195 K was the dihydrogen isomer.²⁴ Upon warming at room temperature an equilibrium took place between the $\eta^2\text{-H}_2$ and the *trans*-dihydride isomers. Jia *et al.* determined that for $[\text{RuH}_2(\text{C}_5\text{Me}_5)(\text{dpmm})]^+$ the interconversion between both isomers (the $\eta^2\text{-H}_2$ isomer and the *trans*-dihydride) actually took place above 230 K, favoring the $\eta^2\text{-H}_2$ isomer.²⁵ Jia *et al.* have shown that the $[\text{OsH}_2(\text{C}_5\text{H}_5)(\text{dpmm})]^+$ complex exists in solution as a mixture of *cis*- and *trans*-dihydride isomers.²⁶ Thus there is a possibility that the *cis* species contains a dihydrogen ligand. We will search for the *trans*-dihydride structure in order to determine the relative stability of it with respect to the $\eta^2\text{-H}_2$ isomer. Finally, the transition-state structure of the rotation of the H_2 unit has also been sought in order to quantify the potential energy barrier associated to the rotation of the dihydrogen unit in the $\eta^2\text{-H}_2$ complex.

It was found that the $\eta^2\text{-H}_2$ structure was the most stable of the two obtained. A stable *trans*-dihydride structure was found 4.10 kcal/mol above the dihydrogen one. This difference in energy is high enough to account for the characteristics of the equilibrium between them reported from experiment. As for the rotational barrier, the transition-state structure of the rotation was found to be 4.23 kcal/mol above the dihydrogen isomer. Along with these calculations, the energy of dissociation of H_2 from the complex was calculated to be 22.7 kcal/mol. This

value denotes that the H_2 unit is strongly bound to the metal fragment. Its binding energy is similar to the experimentally determined values and theoretically calculated energies obtained through high-level calculations for complexes of the type $[\text{ML}(\text{CO})_5(\eta^2\text{-H}_2)]$ ($\text{M} = \text{Cr}, \text{Mo}, \text{W}$).^{27,28} The strength of this bond is related to the weakness of the H–H one. In effect, a very low H–H stretching frequency has been determined recently by Chopra *et al.* for the complex $[\text{Ru}(\text{H}-\text{H})(\text{C}_5\text{H}_5)(\text{dpmm})]^+$.²⁹ Structures for these stationary points are depicted in Figure 1, and a selection of geometrical parameters of these structures, along with the equivalent data determined experimentally by means of neutron diffraction, can be found in Table 1.

Two different subjects arise from Table 1. Focusing on the geometry of the chelating ligand, it can be seen that our Becke3LYP results and the experimental measurements coming from neutron diffraction are in very good agreement. Consequently, it can be concluded that our modelization has not, in any significant way, altered the environment of the metal atom.

On the other hand, there is a remarkably poor agreement between the experimental values of the H–H and Ru–H distances and the corresponding theoretical results. To be concrete, our theoretical results indicate that the most stable structure (in electronic structure terms) is, in fact, a dihydrogen (distance H–H = 0.888 Å), whereas the structure experimentally detected is clearly an elongated dihydrogen (distance H–H = 1.10 Å).

It could be argued that either this minimum we have found is dependent on the level of calculation or that maybe a further minimum nearer to a stretched dihydrogen structure does exist but has not yet been found in our previous exploration of the PES of this system. To check these two possibilities, further efforts were devoted to scan the potential energy profile for the whole range of H–H distances in order to discover in this way the existence of any further minima. Moreover, this potential energy scan has been carried out at different levels of calculation to quantify the dependence of the results on the calculational method chosen. To begin with, this scan has been carried out at the same level of theory and with the same basis set used up to now. It was then repeated, again at Becke3LYP level but

(23) Conroy-Lewis, F. M.; Simpson, S. J. *J. Chem. Soc., Chem. Commun.* **1987**, 1675.

(24) (a) Chinn, M. S.; Heinekey, D. M. *J. Am. Chem. Soc.* **1987**, *109*, 5865. (b) Chinn, M. S.; Heinekey, D. M. *J. Am. Chem. Soc.* **1990**, *112*, 5166.

(25) (a) Jia, G.; Morris, R. H. *J. Am. Chem. Soc.* **1991**, *113*, 875. (b) Jia, G.; Lough, A. J.; Morris, R. H. *Organometallics* **1992**, *11*, 161.

(26) Jia, G.; Ng, W. S.; Yao, J. *Organometallics* **1996**, *15*, 5039.

(27) González, A. A.; Zhang, K.; Nolan, S. P.; López de la Vega, R.; Mukerjee, S. L.; Hoff, C. D. *Organometallics* **1988**, *7*, 2429.

(28) Dapprich, S.; Frenking, G. *Organometallics* **1996**, *15*, 4547.

(29) Chopra, M.; Wong, K. F.; Jia, G.; Yu, N.-T. *J. Mol. Struct.* **1996**, *379*, 93.

Table 1. Structural Parameters for the complexes $[\text{Ru}(\text{H}\cdots\text{H})(\text{C}_5\text{Me}_5)(\text{dppm})]^+$ (Neutron Diffraction) and $[\text{RuH}_2(\text{C}_5\text{H}_5)(\text{H}_2\text{PCH}_2\text{PH}_2)]^+$ (Theoretical Model)^a

	neutron diffraction ^b	$(\eta^2\text{-H}_2)$ structure (1) ^d	<i>trans</i> -dihydride structure (2) ^d	$(\eta^2\text{-H}_2)$ rotational TS (3) ^d
Ru(C ₅ H ₅) (Diphosphine) Fragment ^e				
Ru–P ^c	2.31	2.350	2.347	2.362
Ru–C (C ₅ H ₅) ^{c,e}	2.23	2.315	2.310	2.305
$\angle\text{P1–Ru–P2}$	71.4(3)	71.8	74.0	71.9
$\angle\text{P1–C1–P2}$	93.6(4)	94.6	97.5	95.3
$\angle\text{Ru–P–C1}^c$	97.5	96.5	94.3	96.1
Ru–H ₂ Fragment				
Ru–H ^c	1.67	1.715	1.613	1.778
H(A)–H(B)	1.10	0.888	2.970	0.827
$\angle\text{H(A)–Ru–H(B)}$	38(1)	30.0	134.0	26.9
$\angle\text{P–Ru–H}^c$	80.2	83.5	71.7	81.1

^a Distances are given in Å, and angles in degrees. For atom numeration see Figure 1. ^b Neutron diffraction data from ref 5a. ^c Averaged data. ^d Numbers in parentheses refer to the appropriate structure in Figure 1. ^e Neutron diffraction data refer to the complex with (C₅Me₅) instead of (C₅H₅).

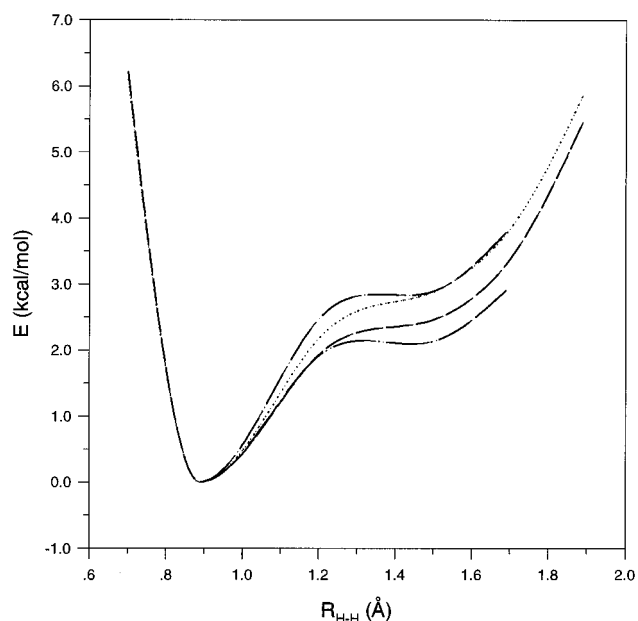


Figure 2. Energy profiles for the lengthening of the H–H bond while relaxing the rest of the structure in the complex $[\text{RuH}_2(\text{C}_5\text{H}_5)(\text{H}_2\text{PCH}_2\text{PH}_2)]^+$, at different calculational levels: (from top to bottom) CCSD/B3LYP (dash-dot), B3LYP*/B3LYP (dot-dot), B3LYP/B3LYP (dash-dash), and CCSD(T)/B3LYP (dash-dot-dot). B3LYP* refers to B3LYP calculations performed with polarization functions on all heavy atoms.

with an enlarged basis set including an *f* shell on the ruthenium atom and *d* shells on all carbon atoms of the model. Finally, a similar scan was carried out again, this time at CCSD and CCSD(T) levels of theory with the original basis set. The calculations carried out with the expanded basis set and at CCSD and CCSD(T) levels were single point calculations performed on Becke3LYP geometries. Figure 2 shows the energy profiles obtained in this way.

As can be seen in Figure 2, there is an excellent accord between the potential energy scans carried out with the original basis set and that with the expanded basis set. Besides, the most striking coincidence comes from calculations at CCSD(T) level, which are very close to those coming from Becke3LYP level. The agreement is so good that the conclusion is that the calculations performed at Becke3LYP level with the original basis are of excellent quality. However, this means that no minimum appears, according to electronic structure alone, at the crystallographically determined distance of 1.10 Å. Anyway, the “shoulder” in the potential energy profile present at H–H distances greater than 1.4 Å can be interpreted as an incipient minimum which would have corresponded to a *cis*-

dihydride structure. This *cis*-dihydride structure, in agreement with experiment, is not a minimum within this calculational level.

A set of conclusions can be drawn on the results obtained up to now. First, Becke3LYP calculations with the original basis set correctly describe the geometry of the chelating ligand in the minimum, in this way validating the modelization done and the calculational level chosen. Second, the calculations at Becke3LYP level and with the original basis set are in very good agreement with calculations carried out with expanded basis sets or at higher levels of theory, showing that it is good enough when studying the system at electronic level. And third, no elongated dihydrogen minimum can be found with the calculational levels tested. As a result, it can be said that electronic structure calculations alone cannot account for the experimental geometry of the H₂ unit in this elongated dihydrogen complex, no matter what the level of theory used is. In order to explain the experimental evidence coming from neutron diffraction data, one should go beyond electronic structure calculations.

B. Nuclear Motion Calculations. As has been seen in the preceding part, even electronic calculations corresponding to a high level of theory cannot explain what is seen experimentally. This statement has been made under the assumption that experimental geometries detected correspond on a one to one basis to minima in the potential energy surface. This statement is not necessarily true under all circumstances, though. One of the consequences of the quantum nature of nuclei is that, even at 0 K, nuclei are not fixed and, actually, the overall structure of a molecule is vibrating no matter what the value of the temperature is. The answer to what would be the expectable value of a given geometrical parameter *x* in a given vibrational state, is the standard method to evaluate expectation values for properties in quantum mechanics:

$$\langle x \rangle_i = \frac{\langle \Psi_i | \hat{x} | \Psi_i \rangle}{\langle \Psi_i | \Psi_i \rangle} \quad (5)$$

where Ψ_i corresponds to the nuclear wave function in state *i*, and \hat{x} is the quantum mechanical operator associated to the *x* geometrical parameter. In very simple systems, such as a monodimensional harmonic oscillator, the value of $\langle x \rangle_i$ matches the position of the minimum in the potential energy surface. However, for potential energy profiles more realistic for chemical problems, such as a Morse potential, the expected position of the particle can be shown to be away from the minimum in the PES. Of course, this deviation of the expected value of the position in a given vibrational state from the minimum in the PES has nothing to do with temperature. It is

a property inherent to a quantum system. At 0 K the system would be confined to the ground vibrational state but, even then, the expected value of the position would be away from the minimum in the PES. Usually, for profiles not very anharmonic and low temperatures, the expected value of the nuclear position is very close to the minimum in the PES. However, as was seen in the previous subsection, the profile corresponding to the lengthening of the H–H bond in our system is *very* anharmonic. As a consequence of this anharmonicity, vibrational wave functions will probably lead to a longer average H–H distance, the magnitude of this effect depending on the magnitude of the zero-point energy: the higher the zero-point vibrational energy is, the longer the H–H distance is. With this in mind, steps have been taken to evaluate the vibrational energy levels and wave functions.

The main interest is centered on the dynamics of the Ru–H₂ unit of the complex. If the results had to be accurate enough, special attention had to be devoted to the dynamical treatment of this part of the complex. The first point to address, and the most costly in computational terms, is the evaluation of the PES part corresponding to the motion of the Ru–H₂ unit. The most important geometrical parameters involved in its dynamics (within C_s symmetry point group) are the H–H distance and the metal center of the dihydrogen unit distance. These two parameters, as described in section II.B, behave as orthogonal geometric parameters. This implies a minimum of two dimensions to describe the dynamics of this unit if these degrees of freedom are to be treated separately.

A third kind of movement of the dihydrogen ligand is also possible: its rotation along the metal center of the dihydrogen axis. However, bearing in mind the relatively high value of the rotational potential energy barrier determined theoretically in section III.A, the rotation of the dihydrogen unit is likely to have little influence on the dynamics of the system. Then, it would be safe to assume that only vibrationally excited states would be affected by this kind of motion.

A two-dimensional (2D) potential energy surface was constructed, then, through evaluation of a collection of 80 points, each corresponding to a different set of H–H and Ru–H₂ distances, and allowing at each of these points the relaxation of the rest of the structure. The ranges covered were from 0.59 to 2.29 Å for the H–H distance, and from 1.00 to 2.20 Å for the Ru–H₂ distance. To better describe the low-energy zones of the PES, a greater number of points were allocated there. Finally, these energetic data were fitted into a set of 2D cubic splines in order to have a useable functional form to solve (2).³⁰ It has to be noted that the lowest energy along the borders of the surface was of ~10.0 kcal/mol, which means that only vibrational energy levels obtained below this value would be reliably determined. Figure 3 depicts the whole bidimensional potential energy surface as a contour plot.

In section III.A it was seen that the monodimensional potential energy profile of the lengthening of the H–H distance presented a kind of “shoulder” corresponding to the incipient—but nonexistent—potential energy minimum in the range of distances corresponding to a dihydride ($R_{\text{H-H}} > 1.4$ Å). Upon examining Figure 3, it can be seen that the potential energy minimum is nothing more than the deepest point in a long valley with smooth slopes in a direction corresponding mainly to the lengthening of the H–H distance, but with a component of decreasing Ru–H₂ distances. A second, steeper exit of this valley exists when the H–H distance is 0.80 Å approximately, which corresponds

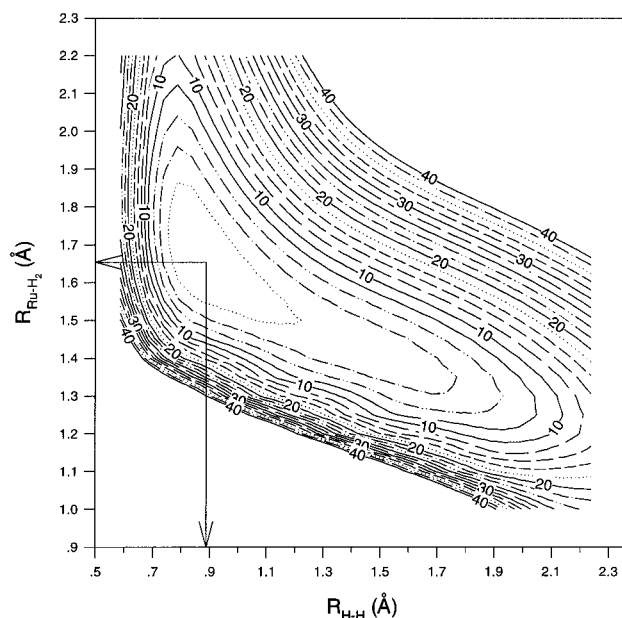


Figure 3. Contour plot of the 2D PES for the complex [RuH₂(C₅H₅)(H₂-PCy₂PH₂)]⁺. Energy contours appear every 2 kcal/mol. The arrows indicate the position of the minimum in potential energy ($R_{\text{H-H}} = 0.89$ Å, $R_{\text{Ru-H}_2} = 1.66$ Å).

to the complex emitting H₂. From the results in section III.A, an asymptotic limit at 22.7 kcal/mol has been determined for this second exit.

Once the 2D PES has been built up, it is time to solve (2) by means of the DVR technique by constructing the matrix representation of the Hamiltonian corresponding to the nuclear motion over a grid of equally spaced points.^{20b} Strictly speaking, a certain mass should be assigned to each degree of freedom in the Hamiltonian in (2). In our case, the fact that the geometries have been allowed to relax at each point makes the assignment of masses to the two degrees of freedom unclear. Despite this fact, single-point unoptimized calculations in which the whole complex except the H₂ unit was frozen to the geometry of the absolute minimum differed little in energy from the corresponding structures optimized and whose energy is represented in Figure 3 (less than 1 kcal/mol difference in the low-energy zones of the PES). In this way, the corresponding reduced masses associated with both axes were assumed to be

$$\frac{1}{\mu_{R_{\text{H-H}}}} = \frac{1}{m_{\text{H(A)}}} + \frac{1}{m_{\text{H(B)}}}$$

$$\frac{1}{\mu_{R_{\text{Ru-H}_2}}} = \frac{1}{m_{\text{H}_2}} + \frac{1}{m_{[\text{RuCp}(\text{H}_2\text{PCH}_2\text{PH}_2)]}} \quad (6)$$

With the corresponding masses assigned, the matrix representation of the Hamiltonian over a rectangular grid of points was constructed and diagonalized. The characteristics of the grid were as follows: 56 points in the $R_{\text{H-H}}$ coordinate and 39 points in the $R_{\text{Ru-H}_2}$ direction, yielding a grand total of 2184 points. Table 2 contains a summary of the results regarding the nuclear energy levels which are 5 kcal/mol above the ground state, for several isotopic varieties of the complex under study, along with expectation values for both geometric parameters.

Maybe the most important result of the vibrational motion calculations performed is kept within the vibrational wave function, which deserves a more thorough analysis. Figure 4 depicts a contour plot of $|\Psi|^2$ for the vibrational ground state

(30) Press, W. H.; Teukolsky, S. A.; Vetterling, W. T.; Flannery, B. P. *Numerical Recipes in FORTRAN*, 2nd ed.; Cambridge University Press, 1992.

Table 2. Vibrational Energy Levels and Expectation Values for Geometrical Parameters in the Ground Vibrational State for Different Isotopomers of the Model Complex^a

energy level	H–H	H–D	D–D	T–T
0	4.58	3.92	3.28	2.68
1	6.15	5.32	4.60	3.87
2	7.58	6.41	5.44	4.57
3	9.09	7.67	6.44	5.32
4			7.50	6.14
5			7.92	6.53
6				7.04
7				7.68
ground state				
$\langle R_{\text{H-H}} \rangle$	1.02	0.99	0.96	0.93
$\langle R_{\text{Ru-H}_2} \rangle$	1.61	1.62	1.63	1.64

^a Only levels within 5 kcal/mol of the vibrational ground state are reported. Energies are given in kcal/mol and distances in Å. Energies are relative to the minimum in the PES.

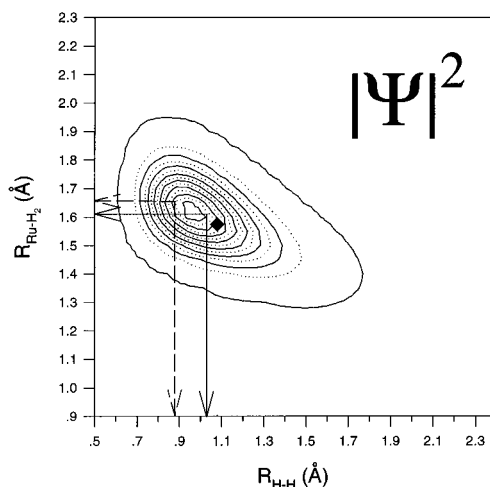


Figure 4. Probability density plot of the vibrational ground-state wave function of complex $[\text{RuH}_2(\text{C}_5\text{H}_5)(\text{H}_2\text{PCH}_2\text{PH}_2)]^+$ as a contour plot of $|\Psi|^2$. The dashed arrow indicates the position of the minimum in the PES ($R_{\text{H-H}} = 0.89 \text{ \AA}$, $R_{\text{Ru-H}_2} = 1.66 \text{ \AA}$), the solid arrow that of the expectation values for this vibrational state ($R_{\text{H-H}} = 1.02 \text{ \AA}$, $R_{\text{Ru-H}_2} = 1.61 \text{ \AA}$), and the square mark, that of the experimentally reported data from neutron diffraction ($R_{\text{H-H}} = 1.10 \text{ \AA}$, $R_{\text{Ru-H}_2} = 1.58 \text{ \AA}$).

of $[\text{Ru}(\text{H}\cdots\text{H})(\text{C}_5\text{H}_5)(\text{H}_2\text{PCH}_2\text{PH}_2)]^+$. As can be seen, the wave function is notably delocalized, encompassing the whole valley in the potential energy surface with nonnegligible values of probability density. This is a direct consequence of the value of the zero-point energy found (4.58 kcal/mol), which places the first energy state above the “shoulder” of potential energy previously mentioned. There are important implications in these results: the shape of the vibrational ground-state wave function implies that the $\eta^2\text{-H}_2$ unit is greatly delocalized. As a consequence, the $\eta^2\text{-H}_2$ unit can no longer be envisaged as a fixed, rigid block. Besides, the most striking result is plainly stated in Figure 4: the most probable localization of the $\eta^2\text{-H}_2$ unit in terms of H–H and Ru–H₂ distances (i.e., the maximum in $|\Psi|^2$) is substantially different from the one predicted by electronic structure calculations alone. Anyway, the value reported experimentally should be compared not with the most probable distances, but with the expectation values calculated through use of (5). The expectation values obtained for both parameters ($\langle R_{\text{H-H}} \rangle = 1.02 \text{ \AA}$, $\langle R_{\text{Ru-H}_2} \rangle = 1.61 \text{ \AA}$) are in much better agreement with neutron diffraction data ($R_{\text{H-H}} = 1.10 \text{ \AA}$, $R_{\text{Ru-H}_2} = 1.58 \text{ \AA}$)^{5a} than are the structural parameters corresponding to the PES minimum ($R_{\text{H-H}} = 0.89 \text{ \AA}$, $R_{\text{Ru-H}_2} = 1.66 \text{ \AA}$). Judging from this fact, it can be said that the quantum nature of nuclei has to be considered to explain certain

Table 3. Mean Thermal Hydrogen–Hydrogen Distances and $J(\text{H,D})$ Coupling Constants as a Function of Temperature

<i>T</i> (K)	thermal		$J(\text{H,D})$ (Hz)	
	$\langle R_{\text{H-H}} \rangle$ (Å)	$\langle R_{\text{H-D}} \rangle$ (Å)	(experimental) ^a	(theoretical)
213	1.030	1.003	22.3	23.4
233	1.033	1.006	22.0	23.2
253	1.035	1.009	21.6	23.1
273	1.038	1.013	21.5	22.9
295	1.042	1.017	21.1	22.6

^a Data for complex $[\text{Ru}(\text{H}\cdots\text{D})(\text{C}_5\text{Me}_5)(\text{dppm})]^+$ from ref 5a.

kinds of phenomena which cannot be understood with reasons based only on electronic structure.

On the other hand, zero-point energy levels depend on the kind of isotopic substitution made on the molecules, and they become lower when heavier isotopes are used. Hence, isotopic substitutions in the dihydrogen ligand may produce notable changes in the zero-point energy level of our system, which in turn would imply changes in the expectation values of these geometrical parameters. The two last rows of Table 3 contain the expectation values for the two geometrical parameters involved in different isotopic variants of our system. As expected, hydrogen–hydrogen distances in the different isotopic species studied are dependent on the isotopic substitution performed. Experiments devoted to confirm this point would be, of course, very interesting and acknowledged.

The final point to be addressed in this paper is to explain the temperature dependence of the hydrogen–hydrogen distances, which is indirectly determined experimentally by means of $J(\text{H,D})$ coupling constant measurements. It has to be noted that experimentally it has been assumed that hydrogen–hydrogen distances are not dependent on isotopic substitution and, hence, that H–H distances are essentially the same that H–D obtained through $J(\text{H,D})$ coupling constant measurements. In order to determine values for the coupling constant, the following procedure has been adopted: the expectation values for both geometrical parameters have been obtained for all the energy levels 5 kcal/mol above the ground state. Then, mean hydrogen–hydrogen distances have been obtained at different temperatures by assuming a Boltzmann-type equilibrium distribution for all the vibrational states considered:

$$\langle x \rangle = \frac{\sum_{E_i < E_0 + 5} \langle x \rangle_i e^{-E_i/RT}}{\sum_{E_i < E_0 + 5} e^{-E_i/RT}} \quad (7)$$

where $\langle x \rangle_i$ refers to the value of the H–H (H–D) distance in the *i*th vibrational state. Mean H–H (H–D) distances were then converted to their $J(\text{H,D})$ coupling constant value by means of empirical relation 1. It should be noted that, according to the results presented in this paper, the inner distance in the dihydrogen ligand depends on the isotopic composition of this same ligand. Table 3 shows the results concerning mean thermal H–H and H–D distances.

As can be seen in Table 3, there are noticeable differences between mean H–H and H–D distances. As expected, mean thermal H–D distances are shorter than the corresponding mean thermal H–H ones. Owing to the fact that the H–D system has a lower zero-point energy level, its vibrational ground-state wave function is more localized near the PES minimum than its corresponding H–H homologue. Apart from that, it can be seen that both mean thermal H–H and H–D distances increase with temperature. This is due to the fact that, at higher temperatures, the population of the vibrationally excited states

of these systems, which have larger mean H–H and H–D distances respectively, is higher.

Now it is possible to evaluate values of $J(\text{H,D})$ coupling constants through use of empirical relation (1). It has to be borne in mind that this relation was determined by relating H–H distances coming from neutron diffraction, X-ray diffraction, and solid-state NMR data, with $J(\text{H,D})$ coupling constant values.^{5b} It was then implicitly assumed that the hydrogen–hydrogen distance is invariant with isotopic substitution. However, as our results indicate, this distance is, in fact, dependent on the type of isotopic substitution done. In this way it can be said that empirical relation (1) not merely relates H–H distances with $J(\text{H,D})$ coupling constant values, but it also somehow takes into account in an indirect way isotopic effects. The last two columns in Table 3 present, then, both the $J(\text{H,D})$ coupling constant coming from experiment and $J(\text{H,D})$ values calculated through use of relation 1 by using H–H (as opposed to H–D) distances.

The values of the $J(\text{H,D})$ coupling constant obtained in this way are systematically higher than experimental ones. This was expected because the expectation values of the H–H distance in the ground vibrational state predicted by our calculations are somewhat shorter than the experimentally reported value, producing a higher $J(\text{H,D})$ coupling constant value. The variation of $J(\text{H,D})$ coupling constant values as a function of temperature is in good agreement with experimental data available, as can be seen in Table 3, in this way confirming that the nuclear motion calculations as a whole are accurate.

IV. Conclusions

In this paper a study of the elongated dihydrogen complex $[\text{Ru}(\text{H}\cdots\text{H})(\text{C}_5\text{H}_5)(\text{H}_2\text{PCH}_2\text{PH}_2)]^+$ has been carried out, taken as a realistic theoretical model of the complex $[\text{Ru}(\text{H}\cdots\text{H})(\text{C}_5\text{Me}_5)(\text{dppm})]^+$. Along with the necessary electronic structure studies, quantum vibrational motion calculations aimed at interpreting the temperature dependence of the $J(\text{H,D})$ coupling constant have also been presented. The discrete variable representation (DVR) formalism has been used to carry out a quantum vibrational motion study. The main conclusions of this work are the following ones.

(1) At the electronic structure level, no minimum corresponding to an elongated dihydrogen structure exists. The experi-

mental geometry cannot be explained with pure electronic structure results.

(2) Quantum vibrational motion calculations finally justify the experimental evidence with regard to geometry, due to the high anharmonicity of the potential. The coupling between the H–H and the Ru–H₂ stretches makes it unrealistic to analyze the vibrational motion in terms of a mere H–H stretch. At least two-dimensional vibrational wave functions are needed to obtain quantitatively valid results.

(3) An isotopic effect on hydrogen–hydrogen distance is foreseen for this complex. The inner dihydrogen distance will become noticeably shorter when heavier isotopes are used in the dihydrogen ligand. Neutron diffraction studies on isotopically substituted variants of the complex under study devoted to proving this prediction would be very interesting.

(4) Our results predict that mean thermal hydrogen–hydrogen distances are dependent on temperature, becoming longer at higher temperatures. This explains the experimentally detected dependence of $J(\text{H,D})$ values on temperature for this complex.

We think that the work we have presented here explains satisfactorily both the experimental structure and the temperature dependence of the $J(\text{H,D})$ coupling constant which are reported for the complex $[\text{Ru}(\text{H}\cdots\text{H})(\text{C}_5\text{Me}_5)(\text{dppm})]^+$. There are, however, several other elongated dihydrogen complexes reported in the literature. At least at a qualitative level, the results we have obtained for this complex should be easily extended to these. Concretely, there is another particularly interesting case, the complex *trans*- $[\text{Os}(\text{H}\cdots\text{H})\text{Cl}(\text{dppe})_2]^+$, for which both neutron diffraction data and $J(\text{H,D})$ coupling constant dependence on temperature data are available.^{5b} In this complex the $J(\text{H,D})$ coupling constant varies inversely with temperature, becoming larger at higher temperatures. Theoretical work is currently underway on this complex in our laboratory along the same lines presented in this paper.

Acknowledgment. Financial support from DGES through projects PB95-0637 and PB95-0639-C02-01 and the use of the computational facilities of the “Centre de Computació i de Comunicacions de Catalunya” are gratefully acknowledged.

JA970838V